A deep root for the Cambrian Explosion: implications of new bio- and chemostratigraphy from the Siberian Platform

Digital Object Identifier (DOI):
10.1130/G38865.1

Geology

A deep root for the Cambrian Explosion: implications of new bio- and chemostratigraphy from the Siberian Platform

--Manuscript Draft--

Manuscript Number:	G38865R1
Full Title:	A deep root for the Cambrian Explosion: implications of new bio- and chemostratigraphy from the Siberian Platform
Short Title:	A deep root for the Cambrian Explosion
Article Type:	Article
Keywords:	Ediacaran; Cambrian Explosion; chemostratigraphy; biostratigraphy; small shelly fossils; carbon isotope excursion; Siberia.
Corresponding Author:	Mao-yan Zhu Nanjing Institute of Geology and Palaeontology, Chinese Academy of Sciences Nanjing, Jiangsu CHINA
Corresponding Author Secondary Information:	
Corresponding Author's Institution:	Nanjing Institute of Geology and Palaeontology, Chinese Academy of Sciences
Corresponding Author's Secondary Institution:	
First Author:	Mao-yan Zhu
First Author Secondary Information:	
Order of Authors:	Mao-yan Zhu
	Andrey Zhuravlev
	Rachel Wood
	Fangchen Zhao
	Sergey Sokhov
Order of Authors Secondary Information:	
Manuscript Region of Origin:	RUSSIAN FEDERATION
Abstract:	Much uncertainty remains as to the temporal relationship between the Ediacaran and Cambrian biotas, yet this is critical to our understanding of the rise of metazoans. Here we present new high resolution carbon isotope chemostratigraphy and biostratigraphy for a terminal Ediacaran to Cambrian succession on the eastern Siberian Platform, Russia, which shows the presence of a succession of diverse fossil assemblages before the start of the basal Cambrian negative carbon isotope excursion (BACE). Soft-bodied Ediacaran biota (Beltanelliformis) occur before the start of the late Ediacaran positive carbon isotope plateau (EPIP), a mixed Ediacaran and Cambrian skeletal biota (Cloudina, Anabarities, Cambrotubulus) appear within the EPIP, and diverse Cambrian-type small shelly fossils including Protohertzina and other protocondonts, halkieriids, chancelloriids, hyoliths, hyolithelminthes and the burrowing trace fossil (Diplocraterion) appear at the beginning of the BACE. These integrated data show that taxa attributed to so-called Ediacaran and earliest Cambrian skeletal biotas in fact overlap without notable biotic turnover, and thus refute the presence of a large isotope excursion coincident with mass extinction of all Ediacaran biota. We propose a new biozone, the Cloudina-Namacalathus-Sinotubulites Assemblage Zone, to precede the known small shelly fossil (SSF) zones. These observations raise doubts as to whether there is any true separation between the Ediacaran and Cambrian skeletal biotas, and suggest that there is a deep root for the Cambrian Explosion of metazoans.
Response to Reviewers:	Many thanks for support from three reviewers that our work will be an excellent contribution to GEOLOGY, and their helpful comments and corrections on our manuscript. We considered the comments carefully and made necessary revisions and

	corrections in text and figures. Major changes and responses to reviewers' comments are listed here, you will find more detail responses to reviews as attached file. 1.The main argument of the reviews (particularly from Reviewer #2) is the age model of the Ust'-Yudoma Formation. The key point is that whether the negative excursion between the Aim and Ust'-Yudoma formations could be the BACE. In fact, a late Ediacaran age for the Ust'-Yudoma formations is not just based on the occurrence of Cloudina, but also based on the integrated correlations from the bio-, chemostratigraphy and sequence stratigraphy of entire Yudoma Group and overlying Pestrotsvet Formation, and their global correlations as stated in detail in the "Discussion". The negative excursions below the Ust'-Yudoma Formation may be of local or regional significance within the terminal Ediacaran carbon isotope plateau, as this is also reported from the equivalent terminal Ediacaran Khatyspyt Formation in NE Siberia (Cui et al., 2016, PPP, 461:122-139). Similar to the Aim Formation, the Khatyspyt Formation also consists of a black limestone with abundant characteristic soft-bodied Ediacara fossils, thus both are a late Ediacaran age below the BACE. Since we resent a short paper, there is no space to add more detailed discussion on the age model for whole sequence and its global correlation. But as Reviewer #1 has pointed out there are no data to suggest a Cambrian age for the Ust'-Yudoma Formation. Reviewer # 3 (Dr. Huan Cui), who has been working on late Ediacaran stratigraphy both in Siberia and South China, indeed has no issue with the proposed age model. But in order to make the point more clearly, we revised relevant part in the "Discussion" and added one new reference (Line 121-142). 2. All three figures were revised in order to meet reviews and size limit. a. Figure 1: We added the unconformity above the Ust'-Yudoma Formation, and replaced symbols on the map. b. Figure 2: We added two more images of Cloudina as requested by Reviewer # 2, and one image of Shaanxilites as requested by Reviewer # 1. Meanwhile, we deleted few images to reduce the size for saving space for text. Subsequent citations in the text and caption in revised. c. Figure 3: Revised the font size in order to meet publication. 3. Because of page limit, the text was condensed and the references were updated. The text was shortened by ca. 940 characters, together with the reduced size of Figure 2, it should meet the four page limit. If printing format is 2 columns as Figure 1 and 3 were prepared with Figure 2 for full page width, I think it would meet page limit.

Publisher: GSA
Journal: GEOL: Geology
DOI:10.1130/G38865.1

A deep root for the Cambrian Explosion: Implications of new bio- and chemostratigraphy from the Siberian Platform

M. Zhu[1,2*], A. Yu. Zhuravlev[3], R.A. Wood[4], F. Zhao[1], and S.S. Sukhov[5]

[1]*State Key Laboratory of Palaeobiology and Stratigraphy, Nanjing Institute of Geology and Palaeontology, Nanjing 210008, China*

[2]*College of Earth Sciences, University of Chinese Academy of Sciences, Beijing 100049, China*

[3]*Department of Biological Evolution, Faculty of Biology, Lomonosov Moscow State University, Leninskie gory 1(12), Moscow 119234, Russia*

[4]*School of GeoSciences, University of Edinburgh, James Hutton Road, Edinburgh EH9 3FE, UK*

[5]*Siberian Scientific Research Institute of Geology, Geophysics and Mineral Resources, Krasny prospekt 67, Novosibisrk 630091, Russia*

*E-mail address: myzhu@nigpas.ac.cn

ABSTRACT

Much uncertainty remains as to the temporal relationship between the Ediacaran and Cambrian biotas, yet this is critical to our understanding of the rise of metazoans. Here we present new high resolution carbon isotope chemostratigraphy and biostratigraphy for a terminal Ediacaran to Cambrian succession on the eastern Siberian Platform, Russia, which shows the presence of a succession of diverse fossil assemblages before the start of the basal Cambrian negative carbon isotope excursion (BACE). Soft-bodied Ediacaran biota (*Beltanelliformis*) occur before the start of the late Ediacaran positive carbon isotope plateau (EPIP), a mixed Ediacaran and Cambrian skeletal biota (*Cloudina*, *Anabarities*, *Cambrotubulus*) appear within the EPIP, and diverse Cambrian-type small shelly fossils including *Protohertzina* and other protocondonts, halkieriids, chancelloriids, hyoliths, hyolithelminthes and the burrowing trace fossil (*Diplocraterion*) appear at the beginning of the BACE. These integrated data show that taxa attributed to so-called Ediacaran and earliest Cambrian skeletal biotas in fact overlap without notable biotic turnover, and thus refute the presence of a large isotope excursion coincident with mass extinction of all Ediacaran biota. We propose a new biozone, the *Cloudina*-*Namacalathus*-*Sinotubulites* Assemblage Zone, to precede the known small shelly fossil (SSF) zones. These observations raise doubts as to whether there is any true separation between the Ediacaran and Cambrian skeletal biotas, and suggest that there is a deep root for the Cambrian Explosion of metazoans.

INTRODUCTION

Diverse soft-bodied and skeletal macroscopic fossils first appeared in the Ediacaran (~575–541 Million years ago (Ma)) and probably represent stem- and crown-group metazoans as well as extinct clades (e.g., Droser and Gehling, 2015). This biota largely disappeared across the Precambrian-Cambrian boundary, which is thought to be marked by the ‘Great Unconformity’ and the basal Cambrian negative carbon isotope excursion (BACE) (e.g. Amthor et al., 2003; Zhu et al., 2006, 2007; Peters and Gaines, 2012). This excursion pre-dates the first appearance of *Treptichnus pedum* (Zhu et al., 2001; Cui et al., 2016; Smith et al., 2016) which defines the Precambrian-Cambrian boundary (Landing, 1994), and marks a major biotic turnover as it was followed by the rapid appearance and diversification of bilaterian animals in the early Cambrian (Erwin et al., 2011). The relationship between the Ediacaran and Cambrian biotas is, however, poorly known, due to the incomplete nature of most successions worldwide, taphonomic bias of fossil preservation, restriction of metazoans to oxygenated habits above an often shallow chemocline, and the difficulty of integrating commonly disparate bio- and chemostratigraphic data. Yet whether these biotas are distinct or related is fundamental to our understanding of the environmental controls on the rise of metazoans.

Here we present new high resolution $\delta^{13}C$ and biostratigraphic data from a highly fossiliferous terminal Ediacaran to Cambrian succession on the distal edge of the eastern Siberian Platform, Russia. This demonstrates for the first time that there was considerable diversification of characteristic Cambrian-type skeletal taxa prior to the BACE. In turn this raises doubts as to whether there is any true separation between the Ediacaran and Cambrian skeletal biotas.

GEOLOGICAL SETTING

We consider the carbon isotope stratigraphy and fossil records at Kyra-Ytyga River, a Ediacaran-Cambrian section on the Yudoma River that formed in the Yudoma-Maya Depression on the southeastern edge of the Siberian Platform (Fig. 1A). This depression shows facies distinct from other well-known Ediacaran-Cambrian transitional successions from the Aldan, Olenek, Kotuy, and Sukharikha rivers (Khomentovsky, 2008; Fig. 1A). The section encompasses the Yudoma Group which is subdivided into the Aim and Ust'-Yudoma formations (Khomentovsky, 2008) (Fig. 1B). The lower Aim Formation (~50 m) is composed of a transgressive systems tract (TST) of basal gray sandstones and red shales, and a highstand systems tract (HST) of the limey dolostones. The upper Aim Formation (~55 m) forms a second sequence and is dominated by dark and finely laminated limestones with thin black shales that represent a the maximum flooding surface followed by black limestone of the HST. The Ust'-Yudoma Formation (~280 m) consists of a third thick sequence of shallow marine massive dolostones, passing transitionally into mixed dolostone and dolomitic limestone at ~180 m from the base, with laminated dolomitic limestone appearing in the final 14 m. The Ust'-Yudoma Formation ends in a regional unconformity and is overlain by the Pestrotsvet Formation in other Yudoma River sections (Khomentovsky, 2008).

CHEMOSTRATIGRAPHY

A near complete high resolution $\delta^{13}C$ chemostratigraphic curve (352 data points) was constructed for ~336 m stratigraphic thickness of the Aim and Ust'- Yudoma formations (Fig. 1B; see *Supplementary Materials*). The basal dolostone of the Aim Formation has $\delta^{13}C$ values of 0–2‰ with a short-lived negative excursion to −0.8‰ occurring at 10 m, then succeeding limestone $\delta^{13}C$ values show a stepped increase to +4‰ before a pronounced negative excursion to −1.2‰ toward the top of the formation coincident with a sequence boundary and major lithological changes. Within the dominantly dolomitic Ust'-Yudoma Formation, $\delta^{13}C$ values rapidly increase to +2.6‰ within < 10 m of the formation base, then show an extensive +1‰ to + 3‰ plateau with a very stable and steady trend gradually increasing to +3‰ by 100 m up-section, then gradually decreasing to +0.5‰ by ~250 m in height from the base of the Ust'-Yudoma Formation showing a consistent fluctuation of 1‰. The final ~45 m of section shows a steady declining trend from +1.7‰ to −0.65‰.

BIOSTRATIGRAPHY

The continuous Kyra-Ytyga River section is characterized by five successive assemblages of fossils, Levels I to V in ascending order (Fig. 1B; See *Supplementary Materials*). Level I is restricted to the laminated limestone of the upper Aim Formation, and includes the Ediacaran soft-bodied *Beltanelliformis brunsae* (Fig. 2U) and ?*Shaanxilithes* (= *Nenoxites*) sp. (Wood et al., 2016; Ivantsov, 2017). Further Ediacaran fossils have been reported from the equivalent interval of the Aim Formation of proximal Yudoma River sections, including *Shaanxilithes* sp. ((Fig. 2W), *Palaeopascichnus* sp., *Suvorovella aldanica*, and *Aspidella terranovica* (Zhuravlev et al., 2009; Wood et al., 2016; Ivantsov, 2017).

The first skeletal fossils appear 183 m from the base of the Ust'-Yudoma Formation (Level II), including *Cloudina* ex gr. *C. riemkeae* (Fig. 2A-C), cloudinids (Fig. 2E), *Anabarites trisulcatus, A. valkovi* (Fig. 2F), and other undetermined SSFs (Fig. 2R) (see also Zhuravlev et al. 2012; Wood et al., 2016).

A small shelly fossil (SSF) assemblage appears 260 m from the base of the Ust'-Yudoma Formation (Level III), dominated by various anabaritids reaching up to 5 mm in tube length (Figs. 2S-T). These fossils are abundant and preserved either as carbonate shells or as casts within the dolostone.

The topmost dolomitic limestone the Ust'-Yudoma Formation is especially rich in SSFs. By 8 m below the top of the formation (Level IV), the fauna is represented by various anabaritids (Figs. 2G-I), cloudinids (Fig. 2D), and protoconodonts (Fig. 2M). The most diverse assemblage appears within the top 4.7 m of the formation (Level V), consisting of anabaritids, orthothecimorph hyoliths, protoconodonts (Figs. 2L, 2N, 2P), halkieriids (Fig. 2Q), *Sachites* sp. (Fig. 2J), siphogonuchitids, chancelloriids (Fig. 2O), hyolithelminthes (Fig. 2K), and the vertical burrowing trace *Diplocraterion* sp. (Fig. 2V).

DISCUSSION

The new $\delta^{13}C$ data provide evidence for a short interval (~50 m) of highly variable isotopic signatures, followed very protracted interval (>275 m) of very stable, positive values. This is interpreted as the late Ediacaran positive carbon isotope plateau (EPIP). Only in the final ~20 m is the start of a negative downturn of the $\delta^{13}C$ values from 1.43 ‰ to −0.65 ‰ recorded. We interpret this to be the start of the BACE based on the following lines of evidence: (1) the continuous Ust'-Yudoma shallow marine carbonate sequence, which underwent very early dolomitization (Wood et al., 2016), shows dominantly stable $\delta^{13}C$ values, and the start of a negative downturn in the absence of any lithological change. We suggest the $\delta^{13}C$ data record an original seawater signature and are thus correlatable with the isotopic plateau recorded in the terminal Ediacaran sequences globally (e.g. Amthor et al., 2003; Zhu et al., 2007; Wood et al., 2015; Smith et al., 2016), (2) the sequence is below the Pestrotsvet Formation unconformity, which occurs above the BACE (Khomentovsky and Karlova, 2005), and (3) a succession of overlapping Ediacaran (in particular cloudinids) and earliest Cambrian skeletal taxa are present prior to this excursion.

The Kyra-Ytyga succession records representative assemblages of both classic Ediacaran and Cambrian fossils. Level 1 yields *Beltanelliformis* and ?*Shaanxilithes* which represent soft-bodied Ediacaran taxa. The *Cloudina-Anabarites* assemblage at Levels II can be interpreted as being uppermost Ediacaran by the presence of *Cloudina*, but *Anabarites* suggests that it can also be attributed to the Nemakit-Daldynian

Anabarites trisulcatus Zone of Siberian stratigraphy. Levels III to V contain various anabaritiids, protoconodonts, halkieriids, chancelloriids, hyolithelminthes, hyoliths as well as vertical burrows are indicative of the *Anabarites trisulcatus* and even *Purella antiqua* zones, which previously only reported in the interval within or above the BACE and below the sub-Tommotian unconformity on the Siberian Platform (Khomentovsky and Karlova, 2005), and are usually considered to be typical of basal Cambrian levels globally (Steiner et al., 2007; Landing et al., 2013; Yang et al., 2016a).

The chemo- and biostratigraphy presented here allows correlation with other regional successions across the Ediacaran − Cambrian transition: many are either relatively condensed or contain significant unconformities (including the Great Unconformity). For example, in northwestern Canada, South China and Kazakhstan a mixed Ediacaran – Cambrian skeletal fauna characterizes the interval above the EPIP and BACE, where the earliest occurrence is close to the nadir of the isotope excursion (Pyle et al., 2006; Yang et al., 2016a). While in Nevada, USA, although both the EPIP and BACE are recorded, the Cambrian-type fossils occur only after the BACE (Smith et al., 2016). The Kyra-Ytyga section therefore provides the only documentation of both Ediacaran and Cambrian skeletal taxa within the EPIP and prior to the BACE. This may be due to the fact that Yudoma Group suffered less erosion during the formation of Great Unconformity in the area (Khomentovsky and Karlova, 2005). Additionally, the preservation of the Ediacaran skeletal fossils is limited to very shallow lithofacies above the oxic chemocline, as found at Kyra-Ytyga (Wood et al., 2016). Ediacaran successions deposited below the chemocline would be expected to lack such faunas.

In sum, these integrated data demonstrate that there was considerable diversification of skeletal metazoans prior to the BACE. Extrapolation of radiometric dating from the South China (Yang et al., 2016b), northern Siberian Platform (Cui et al., 2016), and Oman (Bowring et al., 2007), constrains this transitional skeletal biota to the 545–540 Ma time interval.

The new data show that the Ediacaran and the earliest Cambrian biotas overlapped without any notable biotic turnover (Fig. 3). The BACE can now be constrained to have occurred within the interval of characteristic Cambrian-type skeletal fossil distribution (Fig. 3), thus refuting the presence of a large carbon isotope excursion coincident with the mass extinction of all Ediacaran biota. These observations in turn raise doubts as to whether there is any true separation between the Ediacaran and Cambrian skeletal biotas. Indeed, this contention is supported by the co-occurrence of cloudinids with various skeletal species representing a number of diverse clades of early Cambrian aspect in Siberia, South China, and Kazakhstan (Zhuravlev et al., 2012; Yang et al., 2016a).

Placing the relatively complete Kyra-Ytyga section within a global correlation scheme reveals the need to establish a new SSF biozone. We hence propose the *Cloudina-Namacalathus-Sinotubulites* Assemblage Zone based on the global and additive distribution of these three taxa (Hofmann and Mountjoy, 2001; Zhuravlev et al., 2012), to precede the well-known SSF I (*Anabarites trisulcatus–Protohertzina anabarica*), SSF II (= *Purella antiqua*), and SSF III (= *Watsonella crosbyi*) zones (Steiner et al., 2007; Yang et al., 2016a).

A notable reduction in biodiversity of the soft-bodied Ediacaran biota started at ~550 Ma, with nearly all becoming extinct at the base of the Cambrian (Laflamme et al., 2013). Due to the Great Unconformity, which was diachronous and possibly extended up to at least ~20 Myr duration in the shallow shelf area on the most paleocontinents (Fig. 3), extinction of the soft bodied Ediacaran biota may in fact have been gradual rather than abrupt. To support the 'biotic replacement' model (Laflamme et al., 2013), however, requires further demonstration of competitive or predatory displacement. In conclusion, our new integrated data do not support the contention that extinction of the Ediacaran biota facilitated the Cambrian Explosion, but rather suggest that there is a deep root for the Cambrian Explosion of metazoans.

ACKNOWLEDGMENTS

We thank the Director of Biological Resources and Protected Natural Territories of the Ministry of Nature Protection of the Republic of Sakha (Yakutia), led by Semen Terekhov and the administration of the Ust'-Maya Region for logistical support, and Nikolay Atlasov and Elena Aleksandrova for fieldwork support. MZ and FZ received grants support from the Ministry of Science and Technology of China (2013CB835006), the Chinese Academy of Sciences (XDB18030304), and the National Natural Science Foundation of China. We thank Aleksandr Fedorov and Andrey Ivantsov for supplying images of the fossils, Shuhai Xiao and Guoxiang Li for discussion on the fossils, and Huan Cui and other two anonymous reviewers for helpful suggestions.

REFERENCES CITED

Amthor, J.E., Grotzinger, J.P., Schröder, S., Bowring, S.A., Ramezani, J., Martin, M.W., and Matter, A., 2003, Extinction of *Cloudina* and *Namacalathus* at the Precambrian–

Cambrian boundary in Oman: Geology, v. 31, p. 431–434, doi:10.1130/0091-7613(2003)031<0431:EOCANA>2.0.CO;2.

Bowring, S., Grotzinger, J., Condon, D., Ramezani, J., Newall, M., and Allen, P., 2007, Geochronologic constraints of the chronostratigraphic framework of the Neoproterozoic Huqf Supergroup, Sultanate of Oman: American Journal of Science, v. 307, p. 1097–1145, doi:10.2475/10.2007.01.

Cui, H., Grazhdankin, D.V., Xiao, S., Peek, S., Rogov, V.I., Bykova, N.V., Sievers, N.E., Liu, X.-M., and Kaufman, A.J., 2016, Redox-dependent distribution of early macro-organisms: Evidence from the terminal Ediacaran Khatyspyt Formation in Arctic Siberia: Palaeogeography, Palaeoclimatology, Palaeoecology, v. 461, p. 122–139, doi:10.1016/j.palaeo.2016.08.015.

Droser, M., and Gehling, J.G., 2015, The advent of animals: The view from the Ediacaran: Proceedings of the National Academy of Sciences of the United States of America, v. 112, p. 4865–4870, doi:10.1073/pnas.1403669112.

Erwin, D.H., Laflamme, M., Tweedt, S.M., Sperling, E.A., Pisani, D., and Peterson, K.J., 2011, The Cambrian conundrum: Early divergence and later ecological success in the early history of animals: Science, v. 334, p. 1091–1097, doi:10.1126/science.1206375.

Hofmann, H.J., and Mountjoy, E.W., 2001, *Namacalathus*—*Cloudina* assemblage in Neoproterozoic Miette Group (Byng Formation), British Columbia: Canada's oldest shelly fossils: Geology, v. 29, p. 1091–1094, doi:10.1130/0091-7613(2001)029<1091:NCAINM>2.0.CO;2.

Ivantsov, A.Yu., 2017, On the finds of typical Ediacaran fossils in the Vendian Yudoma Group of eastern Siberia: Doklady Akademii nauk, v. 472, p. 1–4 [in Russian].

Khomentovsky, V.V., 2008, The Yudomian of Siberia, Vendian and Ediacaran systems of the International Stratigraphic Scale: Stratigraphy and Geological Correlation, v. 16, p. 581–598, doi:10.1134/S0869593808060014.

Khomentovsky, V.V., and Karlova, G.A., 2005, The Tommotian Stage base as the Cambrian lower boundary in Siberia: Stratigraphy and Geological Correlation, v. 13, p. 26–40.

Laflamme, M., Darroch, S.A.F., Tweedt, S.M., Peterson, K.J., and Erwin, D.H., 2013, The end of the Ediacara biota: Extinction, biotic replacement, or Cheshire Cat?: Gondwana Research, v. 23, p. 558–573, doi:10.1016/j.gr.2012.11.004.

Landing, E., 1994, Precambrian-Cambrian boundary ratified and a new perspective of Cambrian time: Geology, v. 22, p. 179–182, doi:10.1130/0091-7613(1994)022<0179:PCBGSR>2.3.CO;2.

Landing, E., Geyer, G., Brasier, M.D., and Bowring, S.A., 2013, Cambrian Evolutionary Radiation: Context, correlation, and chronostratigraphy—Overcoming deficiencies of the first appearance datum (FAD) concept: Earth-Science Reviews, v. 123, p. 133–172, doi:10.1016/j.earscirev.2013.03.008.

Peters, S.E., and Gaines, R.R., 2012, Formation of the ‘Great Unconformity’ as a trigger for the Cambrian explosion: Nature, v. 484, p. 363–366, doi:10.1038/nature10969.

Pyle, L.J., Narbonne, G.M., Nowlan, G.S., Xiao, S., and James, N.P., 2006, Early Cambrian metazoan eggs, embryos, and phosphatic microfossils from northwestern

Canada: Journal of Paleontology, v. 80, p. 811–825, doi:10.1666/0022-3360(2006)80[811:ECMEEA]2.0.CO;2.

Smith, E.F., Nelson, L.L., Strange, M.A., Eyster, A.E., Rowland, S.M., Schrag, D.P., and Macdonald, F.A., 2016, The end of the Ediacaran: Two new exceptionally preserved body fossil assemblages from Mount Dunfee, Nevada, USA: Geology, v. 44, p. 911–914, doi:10.1130/G38157.1.

Steiner, M., Li, G., Qian, Y., Zhu, M., and Erdtmann, B.-D., 2007, Neoproterozoic to Early Cambrian small shelly fossil assemblages and a revised biostratigraphic correlation of the Yangtze Platform (China): Palaeogeography, Palaeoclimatology, Palaeoecology, v. 254, p. 67–99, doi:10.1016/j.palaeo.2007.03.046.

Wood, R.A., Poulton, S.W., Prave, A.R., Hoffmann, K.-H., Clarkson, M.O., Guilbaud, R., Lyne, J.W., Tostevin, R., Bowyer, F., Penny, A.M., Curtis, A., and Kasemann, S.A., 2015, Dynamic redox conditions control late Ediacaran metazoan ecosystems in the Nama Group, Namibia: Precambrian Research, v. 261, p. 252–271, doi:10.1016/j.precamres.2015.02.004.

Wood, R., Zhuravlev, A.Yu., Sukhov, S.S., Zhu, M., and Zhao, F., 2016, Demise of Ediacaran dolomitic seas marks widespread biomineralisation on the Siberian platform: Geology, v. 45, p. 27–30, doi:10.1130/G38367.1.

Yang, B., Steiner, M., Zhu, M., Li, G., Liu, J., and Liu, P., 2016a, Transitional Ediacaran-Cambrian small skeletal fossil assemblages from South China and Kazakhstan: Implications for chronostratigraphy and metazoan evolution: Precambrian Research, v. 285, p. 202–215, doi:10.1016/j.precamres.2016.09.016.

Yang, C., Li, X.-H., Zhu, M., and Condon, D.J., 2016b, SIMS U-Pb zircon geochronological constraints on the upper Ediacaran stratigraphic correlations, South China: Geological Magazine, p. 1–15, doi:10.1017/S0016756816001102.

Zhu, M.Y., Li, G.X., Zhang, J.M., Steiner, M., Qian, Y., and Jiang, Z.W., 2001, Early Cambrian stratigraphy of east Yunnan, southwestern China: A synthesis: Acta Palaeontologica Sinica, v. 40, p. 4–39.

Zhu, M.-Y., Babcock, L.E., and Peng, S.-C., 2006, Advances in Cambrian stratigraphy and paleontology: Integrating correlation techniques, paleobiology, taphonomy and paleoenvironmental reconstruction: Palaeoworld, v. 15, p. 217–222, doi:10.1016/j.palwor.2006.10.016.

Zhu, M., Strauss, H., and Shields, G.A., 2007, From Snowball Earth to the Cambrian bioradiation: Calibration of Ediacaran-Cambrian Earth history in South China: Palaeogeography, Palaeoclimatology, Palaeoecology, v. 254, p. 1–6, doi:10.1016/j.palaeo.2007.03.026.

Zhuravlev, A. Yu., Gámez Vintaned, J.A., and Ivantsov, A. Yu., 2009, First finds of problematic Ediacaran fossil *Gaojiashania* in Siberia and its origin: Geological Magazine, v. 146, p. 775–780, doi:10.1017/S0016756809990185.

Zhuravlev, A.Yu., Liñán, E., Gámez Vintaned, J.A., Debrenne, F., and Fedorov, A.B., 2012, New finds of skeletal fossils in the terminal Neoproterozoic of the Siberian Platform and Spain: Acta Palaeontologica Polonica, v. 57, p. 205–224, doi:10.4202/app.2010.0074.

FIGURE CAPTIONS

Figure 1. The Yudoma Group, Kyra–Ytyga River section, Yudoma River, with inset map of the Siberian Platform, Russia. A: Map of the Siberian Platform showing structural-facies regions (modified after Khomentovsky, 2008; F1a – Uchur-Maya Plate and F1b – Yudoma-Maya Depression, F2 – Lena-Aldan, F3 – Baykal-Lena, F4 – Enisey-Angara, F5a – Igarka-Noril'sk Uplift, F5b – Anabar Uplift, and F5c – Olenek Uplift), the Yudoma River sections (1 – Kyra-Ytyga River, 2 – Nuuchchalakh valley, 3 – Yudoma-Maya confluence) and the well-investigated transitional Ediacaran-Cambrian sections (4 – Dvortsy, Aldan River, 5 – Olenek and Khorbusuonka rivers, 6 – Bol'shay and Malaya Kuonamka rivers, 7 – Sukharikha River). B: Stratigraphic log, carbon isotope chemostratigraphy, and fossil distribution. Levels I, II, III, IV and V mark the fossil horizons of the section.

Figure 2. Fossils from the Kyra-Ytyga River section. **A–C:** *Cloudina* ex gr. *C. riemkeae*, Level-II. **D:** cloudinid, Level-IV. **E:** cloudinid, Level-II. **F:** *A. valkovi*, Level-II. **G:** *Anabarites natellus,* Level-IV. **H:** *A. latus,* Level-IV. **I:** *Aculeochrea composita,* Level-IV. **J:** *Sachites* sp., Level-V. **K:** *Hyolithellus tenuis*, Level-V. **L:** *Protohertzina ?anabarica*, Level-V. **M:** *P. unguliformis*, Level-IV. **N:** *Fomitchella acinaciformis,* Level-V. **O:** chancelloriid, Level-V. **P:** *Fomitchella infundibuliformis*, Level-V. **Q:** *Halkieria* sp., Level-V. **R:** undetermined shelly fossils, Level-II. **S:** anabaritid packstone, Level-III. **T:** 1, *Anabarites trisulcatus*, b, *A. latus*; Level-III. **U:** *Beltanelliformis brunsae*, Level-I. **V:** *Diplocraterion* sp., Level-V. **W:** *Shaanxilites* sp., from the Aim Formation at Nuuchchalakh valley. Photography: **A–R** – Aleksandr Fedorov, **(U)** – Andrey Ivantsov.

Publisher: GSA
Journal: GEOL: Geology
DOI:10.1130/G38865.1

Figure 3. Summary of temporal distribution of the terminal Ediacaran soft-bodied fossils, Ediacaran to Cambrian skeletal fossils, together with general carbon isotope chemostratigraphy (modified after Zhu et al., 2006, 2007 with explanation of the acronyms for the isotope excursions DOUNCE/SHURAM, BASE, SHICE and ZHUCE) and the approximate duration of the Great Unconformity. Current categories of 'Ediacaran-type (E-type)' and 'Cambrian-type' skeletal fossils are shown, with established zones SSF I, II, and III, and the proposed *Cloudina-Namacalathus-Sinotubulites* Assemblage Zone (CNS Zone).

[1]GSA Data Repository item 2017xxx, xxxxxxxx, is available online at www.geosociety.org/datarepository/2017 or on request from editing@geosociety.org.

Figure 1-TIFF

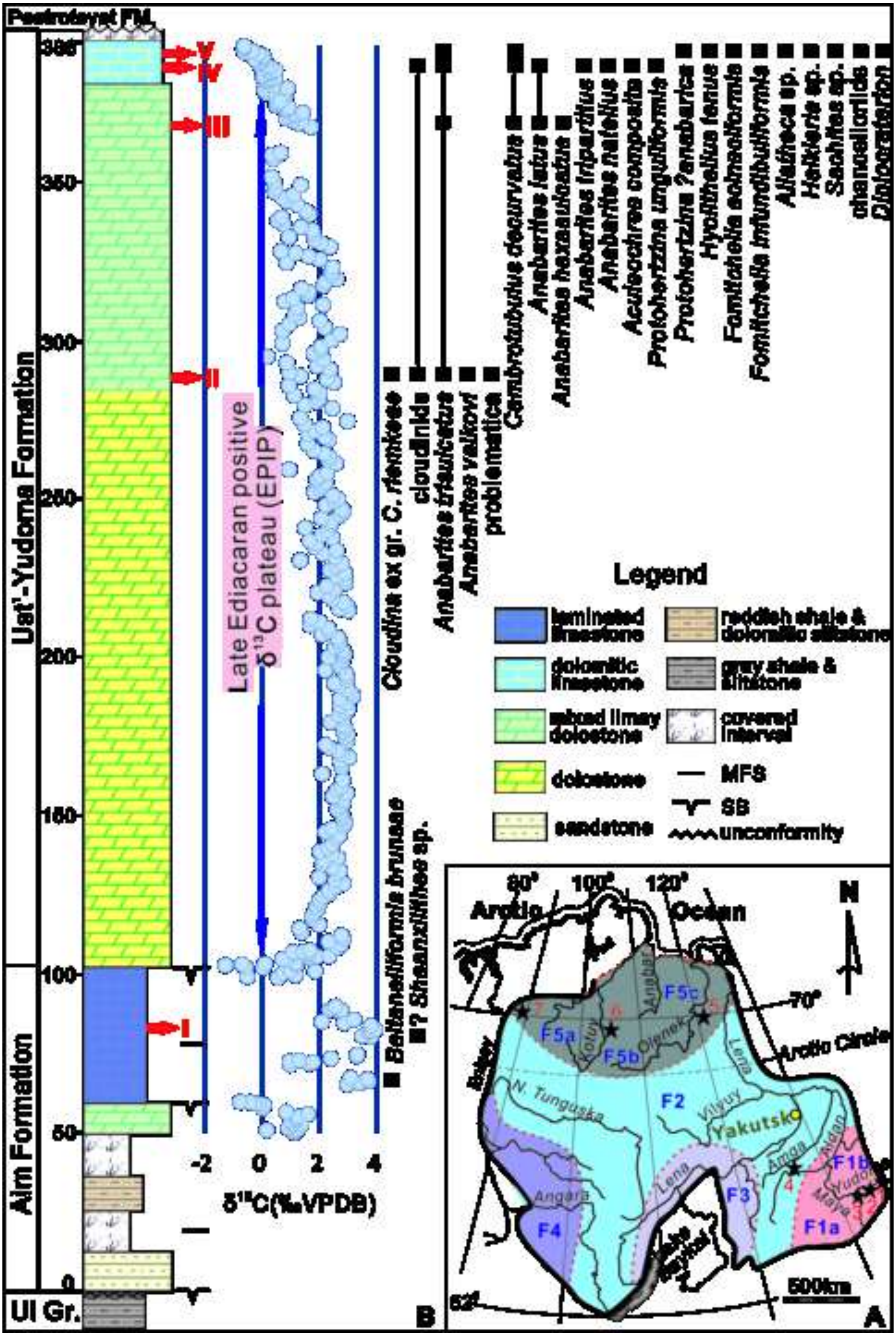

Figure 2-TIFF

Click here to download Figure Zhu et al-Siberia-Fig2-revised-final.tif

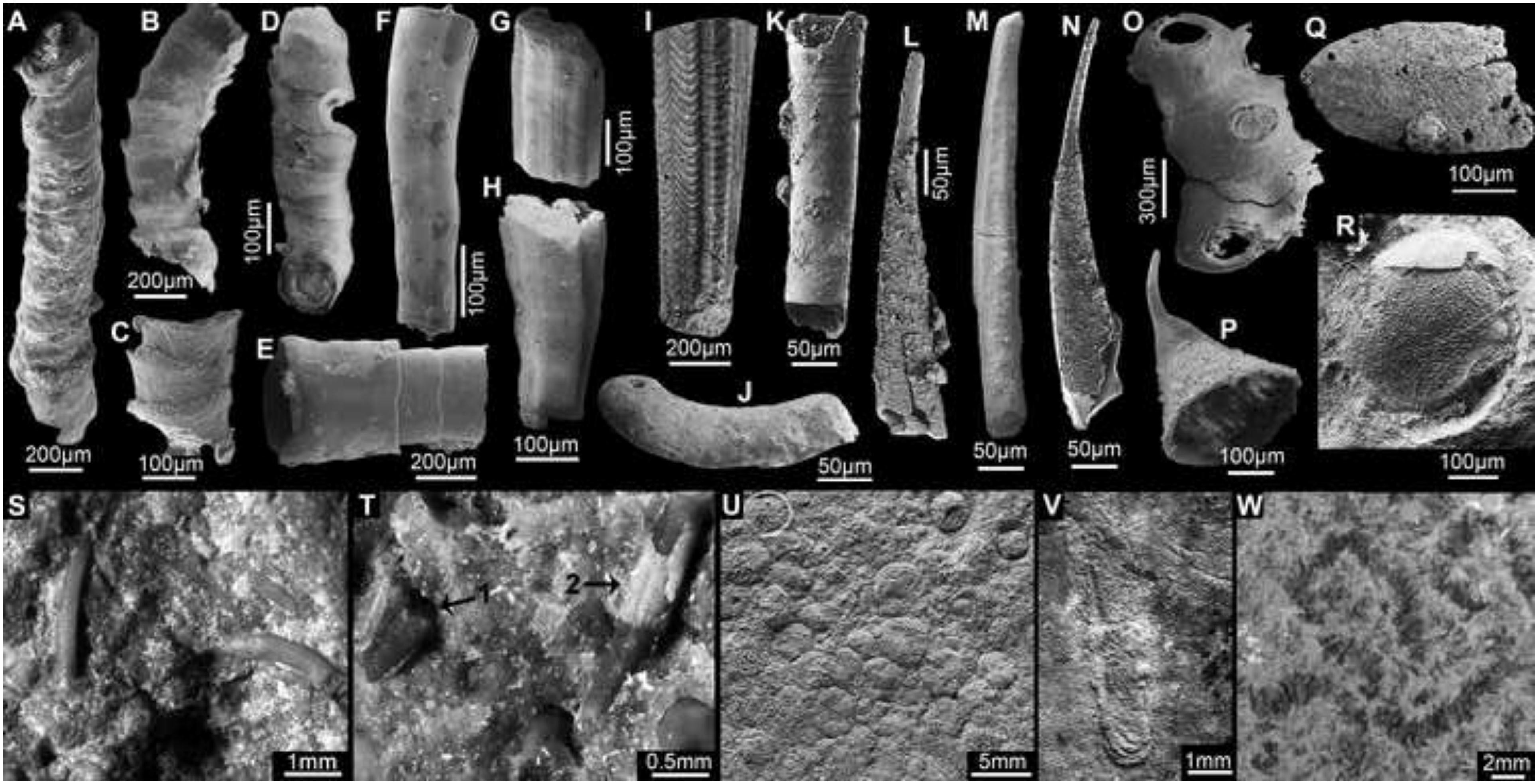

Figure 3-TIFF

Click here to download Figure Zhu et al-Siberia-Fig3-revised-final.tif

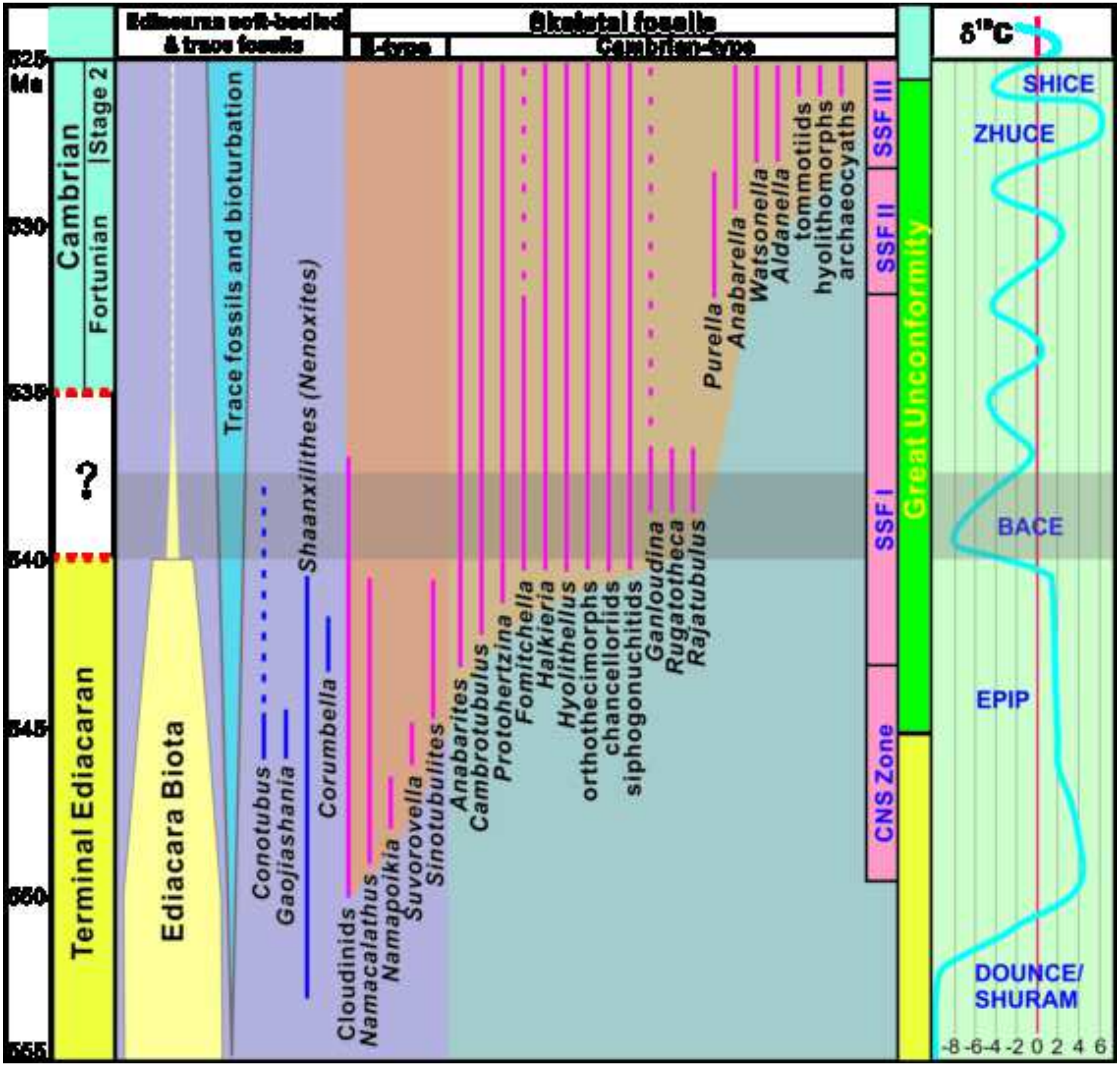

Supplementary Materials

Locality information

Kyra-Ytyga river = 59°29'38.7"N 137°14'41.0"E

List of fossils of the Yudoma Group from sections on the Yudoma River, south-eastern Siberian Platform (Republic of Sakha (Yakutia), Russia

Level I. Aim Formation

1. **Kyra-Ytyga River section:**
    - *Beltanelliformis brunsae* Menner in Keller et al., 1974 – moulds on limy siltstone bedding surfaces, 30.0-45.0 m above the base of the formation, collection A. Ivantsov and A. Zhuravlev, 1998 (?*Nemiana simplex* in Ivantsov et al., 2014, fig. 5; Ivantsov, 2017; Fig. 2U, herein).
    - ?*Shaanxilithes* sp. – imprints on limy siltstone bedding surfaces, 29.5-45.0 m above the base of the formation, collection A. Zhuravlev et al., 2015 (Wood et al., 2016).

2. **Nuuchchalakh valley section:**
    - *Shaanxilithes* sp. (= *Nenoxites* sp.) – imprints on limy siltstone bedding surfaces of black limestone, 80.4-94.5 m above the base of the formation, collection A. Ivantsov and A. Zhuravlev, 1998 (*Gaojiashania annulocosta* in Zhuravlev et al., 2009, fig. 2; *Shaanxilithes* in Cai et al., 2011; *Gaojiashania* in Wood et al., 2016, fig. 2A; *Nenoxites curvus* in Ivantsov, 2017, fig. 2г; Fig. 2W herein).
    - Acritarchs *Leiomarginatasphaera punctulata* Pyatiletov, 1988; *Granomarginatasphaera judomica* Pyatiletov, 1988; *Bailikania diligena* Treshchetenkova, 1981; *"Sibiriella" prima* Fayzulina, 1981; *Bavlinella faveolata* (Shepeleva, 1963) Vidal, 1976; *Leiovalia*

sp.; *Leiosphaeridia rubiginosa* (Andreeva, 1966) Jankauskas et al., 1989; *L. minutissima* (Naumova, 1949) Jankauskas et al. 1989; *L. minuta* (Naumova, 1961) Jankauskas et al., 1989; *Siphonophycus robustum* (Schopf, 1968) Knoll et al., 1991; *S. typicum* (Hermann, 1974) Butterfield et al., 1994 – organic envelops from black siltstone, 11.6-27.6 m above the base of the formation (Pyatiletov, 1988, pls. 1, 2; names are corrected in accordance with current systematics).

3. **Yudoma-Maya confluence section:**

- *Beltanelliformis brunsae* Menner in Keller et al., 1974 – moulds on bedding surfaces of black sandstone, 11.0-11.3 m above the base of the section, collections A. Ivantsov, 2014; A. Ivantsov and A. Zhuravlev, 2015 (Ivantsov, 2017, fig.2a).
- *Palaeopascichnus* sp. – moulds on bedding surfaces of black sandstone, 11.0-11.3 m above the base of the section, collections A. Ivantsov, 2014; A. Ivantsov and A. Zhuravlev, 2015 (Ivantsov, 2017, fig. 2в).
- *Aspidella terranovica* Billings, 1872 – moulds on bedding surfaces of black sandstone, 11.0-11.3 m above the base of the section, collections A. Ivantsov, 2014; A. Ivantsov and A. Zhuravlev, 2015 (Wood et al., 2016, fig. 2E; Ivantsov, 2017, fig. 2б).
- *Suvorovella aldanica* Vologdin and Maslov, 1960 – complete and fragmented shells in dolomitic shelly packstone, 14.6-16.9 m above the base of the section, collections A. Ivantsov, 2014; A. Ivantsov and A. Zhuravlev, 2015 (*Suvorovella aldanica, Majaella verkhojanica, Majaella* sp. I, and Hyolithoides in Vologdin and Maslov, 1960, fig. 1; *Suvorovella aldanica* and *Cyclomedusa* sp. in Sokolov, 1972, figs. 5, 6; *Suvorovella* sp. and *Cyclomedusa* ex. gr. *plana* in Sokolov, 1976, figs. a, г; Ivantsov, 2016; Wood et al., 2016, fig. 2C).

Level II. Ust'-Yudoma Formation, 183 m above the base

Kyra-Ytyga River section:

- *Cloudina* ex gr. *C. riemkeae* Germs, 1972 – phosphatized tubes from limy dolomitic packstone, collection A. Fedorov, 1981 (Zhuravlev et al., 2012, fig. 3A-E; Wood et al., 2016, fig. 2E; Fig. 2A-C, herein).
- Cloudinids – phosphatized tubes from limy dolomitic packstone, collection A. Fedorov, 1981 (Fig. 2E, herein).
- *Anabarites trisulcatus* Missarzhevsky in Voronova and Missarzhevsky, 1969 – phosphatized steinkerns from limy dolomitic packstone, collection A. Fedorov, 1981 (Wood et al., 2016, fig. 2F).
- *A. valkovi* (Bokova in Bokova and Vasil'eva, 1990) – phosphatized steinkerns from limy dolomitic packstone, collection A. Fedorov, 1981 (Fig. 2F, herein).
- Spaeroid shelly problematica – shells from limy dolomitic packstone, collection A. Fedorov, 1981 (Fig. 2R, herein).
- Megasphaeromorph acritarchs – dolomitized envelopes from dolomitic packstone, collection A. Fedorov, 1981 (Wood et al., 2016, fig. 2D).

Level III. Ust'-Yudoma Formation, 260 m above the base

Kyra-Ytyga River section:

- *Anabarites trisulcatus* Missarzhevsky in Voronova and Missarzhevsky, 1969 – shells and steinkerns from limy dolomitic packstone, collection A. Zhuravlev et al., 2015 (Fig. 2T1, herein).
- *A. latus* (Vail'kov and Sysoev, 1970) – shells and steinkerns from limy dolomitic packstone, collection A. Zhuravlev et al., 2015 (Fig. 2T2, herein).
- *A. hexasulcatus* Missarzhevsky, 1974 – shells and steinkerns from limy dolomitic packstone, collection A. Zhuravlev et al., 2015.

- *Cambrotubulus decurvatus* Missarzhevsky in Rozanov et al., 1969 – shells and steinkerns from limy dolomitic packstone, collection A. Zhuravlev et al., 2015 (Fig. 2S, herein).

Level IV. Ust'-Yudoma Formation, 8 m below the top

Kyra-Ytyga River section:

- *Anabarites trisulcatus* Missarzhevsky in Voronova and Missarzhevsky, 1969 – phosphatized steinkerns from limy dolomitic packstone, collection Yu. Shabanov, 1967.
- *A. latus* (Vail'kov and Sysoev, 1970) – phosphatized steinkerns from limy dolomitic packstone, collection Yu. Shabanov, 1967 (Fig. 2H, herein).
- *A. natellus* (Vail'kov and Sysoev, 1970) – phosphatized steinkerns from limy dolomitic packstone, collection Yu. Shabanov, 1967 (Fig. 2G, herein).
- *A. tripartitus* Missarzhevsky in Rozanov et al., 1969 – phosphatized steinkerns from limy dolomitic packstone, collection Yu. Shabanov, 1967.
- *Aculeochrea composita* (Missarzhevsky in Rozanov et al., 1969) – phosphatized steinkerns from limy dolomitic packstone, collection Yu. Shabanov, 1967 (Fig. 2I, herein).
- *Cambrotubulus decurvatus* Missarzhevsky in Rozanov et al., 1969 – phosphatized steinkerns from limy dolomitic packstone, collection Yu. Shabanov, 1967.
- Cloudinids – phosphatized tubes from limy dolomitic packstone, collection Yu. Shabanov, 1967 (Fig. 2D, herein).
- *Protohertzina unguliformis* Missarzhevsky, 1973 – phosphatic shells from limy dolomitic packstone, collection Yu. Shabanov, 1967 (Fig. 2M, herein).

Level V. Ust'-Yudoma Formation, 4.7 m below the top

Kyra-Ytyga River section:

- *Anabarites trisulcatus* Missarzhevsky in Voronova and Missarzhevsky, 1969 – phosphatized steinkerns from limy dolomitic packstone, collection Yu. Shabanov, 1967.
- *Cambrotubulus decurvatus* Missarzhevsky in Rozanov et al., 1969 – phosphatized steinkerns from limy dolomitic packstone, collection Yu. Shabanov, 1967.
- *Protohertzina ?anabarica* Missarzhevsky, 1973 – phosphatic shells from limy dolomitic packstone, collection Yu. Shabanov, 1967 (Fig. 2L, herein).
- *Fomitchella acinaciformis* Missarzhevsky in Rozanov et al., 1969 – phosphatic shells from limy dolomitic packstone, collection Yu. Shabanov, 1967 (Fig. 2N, herein).
- *F. infundibuliformis* Missarzhevsky in Rozanov et al., 1969 – phosphatic shells from limy dolomitic packstone, collection Yu. Shabanov, 1967 (Fig. 2P, herein).
- *Halkieria* sp. – phosphatized steinkerns from limy dolomitic packstone, collection Yu. Shabanov, 1967 (Fig. 2Q, herein).
- *Sachites* sp. – phosphatized steinkerns from limy dolomitic packstone, collection Yu. Shabanov, 1967 (Fig. 2J, herein).
- Chancelloriid – phosphatized steinkern from limy dolomitic packstone, collection V. Khomentovsky, 1967 (Fig. 2O, herein).
- *Hyolithellus tenuis* Missarzhevsky in Rozanov and Missarzhevsky, 1966 – phosphatic tubes from limy dolomitic packstone, collection Yu. Shabanov, 1967 (Fig. 2K, herein).
- Siphogonuchitid – phosphatized steinkern from limy dolomitic packstone, collection Yu. Shabanov, 1967.
- *Allatheca* sp. – calcareous shells from limy dolomitic packstone, collection A. Zhuravlev et al., 2015.
- *Diplocraterion* sp. – vertical burrowing trace fossil from limy dolomitic packstone, collection A. Zhuravlev et al., 2015 (Fig. 2V, herein).

REFERENCES CITED

Cai, Y., Hua, H., Zhuravlev, A.Yu., Gámez Vintaned, J.A., and Ivantsov, A. Yu., 2011, Discussion of 'First finds of problematic Ediacaran fossil *Gaojiashania* in Siberia and its origin': Geological Magazine, v. 148, p. 329–333, doi:10.1017/S0016756810000749.

Ivantsov, A.Yu., 2017, On the finds of typical Ediacaran fossils in the Vendian Yudoma Group of eastern Siberia: Doklady Akademii nauk, v. 472, p. 1–4 [in Russian].

Ivantsov, A.Yu., Gritsenko, V.P., Konstantinenko, L.I., and Zakrevskaya, M.A., 2014, Revision of the problematic macrofossil *Beltanelliformis* (=*Beltanella, Nemiana*): Paleontological Journal, v. 48, p. 1423–1448, doi: 10.1134/S0031030114130036.

Pyatiletov, V.G., 1988, Late Precambrian microfossils of the Uchur-Maya Region, in Khomentovsky, V.V., and Shenfil', V.Yu., eds., Late Precambrian and Early Palaeozoic of Siberia, Riphean and Vendian, Collection of Scientific Papers: Institute of Geology and Geophysics, Siberian Branch, USSR Academy of Sciences, Novosibirsk, p. 47–104 [in Russian].

Sokolov, B.S., 1972, The Vendian Stage in the Earth history, in International Geological Congress, 27th Session, Reports of Soviet Geologists, Problem 7, Paleontology: Nauka, Moscow, p. 114-124 [in Russian].

Sokolov, B.S., 1976, Organic world on the Earth at the approach of the Phanerozoic differentiation: Vestnik Akademii nauk SSSR, v. 1, p. 126–143 [in Russian].

Vologdin, A.G., and Maslov, A.B., 1960, On a new group of fossil organisms from the lower Yudoma Formation of the Siberian Platform: Doklady Akademii nauk SSSR, v. 134, p. 691–693 [in Russian].

Wood, R. Zhuravlev, A.Yu., Sukhov, S.S., Zhu, M., and Zhao, F., 2016, Demise of Ediacaran dolomitic seas marks widespread biomineralisation on the Siberian platform: Geology, doi:10.1130/G38367.1.

Zhuravlev, A.Yu., Gámez Vintaned, J.A., and Ivantsov, A. Yu., 2009, First finds of problematic Ediacaran fossil *Gaojiashania* in Siberia and its origin: Geological Magazine, v. 146, p. 775–780, doi:10.1017/S0016756809990185.

Zhuravlev, A.Yu., Liñán, E., Gámez Vintaned, J.A., Debrenne, F., and Fedorov, A.B., 2012, New finds of skeletal fossils in the terminal Neoproterozoic of the Siberian Platform and Spain: Acta Palaeontologica Polonica, v. 57, p. 205–224, doi:10.4202/app.2010.0074.

Carbon and Oxygen isotope data of the Kyra-Ytyga section

Stratigraphic height (m) of samples starts from the first carbonate at the middle of the Aim Formation of the section. Microdrilling samples of carefully selected micritic carbonate were analysed for $\delta^{13}C$ and $\delta^{18}O$ data simultaneously by a Thermo Scientific MAT-253 mass spectrometer with Kiel IV Carbonate Device at the State Key Laboratory of Palaeobiology and Stratigraphy, Nanjing Institute of Geology and Palaeontology, Chinese Academy of Sciences. Carbonate $\delta^{13}C$ and $\delta^{18}O$ isotopic results are reported in per mil (‰) notation relative to VPDB (Vienna Peedee belemnite). Standard deviation is better than 0.03 ‰ for $\delta^{13}C$ and 0.08 ‰ for $\delta^{18}O$ based on the national standard (Reference number GBW 04405).

Samples	Height(m)	$\delta^{13}C_{PDB}$	$\delta^{18}O_{PDB}$
KY0	0	1.137	-6.369
KY0.2	0.2	1.091	-6.045
KY0.5	0.5	1.184	-6.332
KY0.8	0.8	0.170	-7.666
KY1	1	1.234	-5.168
KY1.5	1.5	0.915	-7.800
KY1.9	1.9	1.074	-7.794
KY2.55	2.55	1.373	-1.221
KY2.8	2.8	1.094	-7.041
KY3.5	3.5	1.004	-3.844
KY4	4	1.191	-9.719
KY4.6	4.6	1.203	-4.623
KY5	5	1.290	-8.882
KY5.8	5.8	1.605	-8.349
KY6.5	6.5	0.848	-10.900
KY7.6	7.6	0.029	-7.663
KY8.5	8.5	0.069	-7.651
KY9	9	-0.102	-8.032
KY9.1	9.1	-0.269	-9.557
KY9.4	9.4	-0.418	-9.793
KY9.5	9.5	-0.753	-9.333
KY15	15	2.977	-7.958
KY15.4	15.4	3.407	-8.092
KY16	16	3.732	-6.826
KY16.5	16.5	3.676	-7.169
KY17	17	3.095	-7.436
KY21	21	0.984	-7.764
KY21.4	21.4	1.650	-7.290
KY21.9	21.9	1.780	-7.143
KY22.1	22.1	0.975	-7.084
KY22.4	22.4	1.307	-6.768
KY23	23	2.416	-7.162
KY23.7	23.7	3.308	-6.817
KY24.2	24.2	3.319	-6.946
KY29.7	29.7	3.801	-5.801

KY30	30	3.502	-6.705
KY31	31	3.710	-5.502
KY31.3	31.3	3.784	-6.222
KY31.4	31.4	3.812	-6.231
KY31.9	31.9	3.950	-5.631
KY33.1	33.1	3.806	-5.731
KY34	34	2.871	-6.407
KY34.3	34.3	2.091	-5.949
KY35	35	3.207	-5.444
KY37.5	37.5	2.685	-6.066
KY37.7	37.7	2.676	-5.833
KY37.8	37.8	2.763	-5.848
KY38	38	2.357	-6.047
KY38.5	38.5	2.488	-5.770
KY39	39	2.577	-5.859
KY48	48	0.556	-6.054
KY48.3	48.3	-0.515	-5.553
KY48.8	48.8	1.162	-7.308
KY49.3	49.3	0.728	-6.504
KY49.9	49.9	0.993	-6.398
KY50	50	1.859	-6.881
KY51	51	0.040	-6.929
KY51.3	51.3	-0.575	-6.875
KY51.8	51.8	-1.273	-7.025
KY52	52	1.202	-7.107
KY52.1	52.1	-0.696	-6.963
KY52.2	52.2	0.106	-6.000
KY52.5	52.5	1.184	-7.416
KY53.3	53.3	0.872	-7.223
KY53.7	53.7	0.728	-7.560
KY54.1	54.1	1.631	-7.726
KY54.5	54.5	1.921	-9.493
KY54.7	54.7	2.342	-10.080
KY55	55	1.570	-12.756
KY55.4	55.4	1.651	-11.929
KY55.5	55.5	1.157	-8.730
KY55.9	55.9	1.086	-7.395
KY56	56	1.443	-7.950
KY56.4	56.4	1.673	-6.645
KY57.3	57.3	2.639	-10.949
KY58.1	58.1	2.741	-9.906
KY59.1	59.1	2.322	-7.898
KY59.9	59.9	2.838	-10.053
KY61	61	2.764	-11.199
KY62	62	1.382	-10.798
KY63.2	63.2	1.318	-9.710
KY64.4	64.4	1.995	-8.463
KY66	66	1.779	-8.193
KY67	67	1.743	-8.103
KY68	68	1.829	-7.987
KY69	69	1.931	-8.265
KY70	70	1.910	-7.794
KY71	71	2.013	-8.976
KY72	72	2.017	-8.097
KY73	73	2.135	-7.925
KY74	74	2.347	-9.267
KY75	75	2.338	-9.916

KY76	76	2.571	-8.943
KY77	77	2.837	-8.496
KY78	78	2.556	-10.992
KY79	79	1.990	-10.268
KY80	80	2.625	-10.173
KY81	81	2.723	-9.483
KY82	82	2.456	-10.313
KY83	83	2.114	-11.158
KY84	84	2.155	-10.755
KY85	85	2.647	-10.633
KY86	86	2.440	-9.984
KY87	87	2.026	-10.901
KY88	88	2.286	-11.028
KY89	89	2.453	-10.648
KY91	91	2.606	-9.757
KY92	92	2.691	-9.790
KY93	93	2.220	-9.599
KY94	94	2.453	-10.004
KY95	95	2.852	-10.228
KY96	96	2.914	-8.630
KY97	97	2.818	-6.648
KY98	98	2.809	-7.909
KY99	99	2.748	-8.467
KY100	100	2.629	-9.076
KY101	101	2.770	-9.423
KY102	102	2.844	-8.316
KY103	103	2.848	-9.009
KY104	104	2.486	-7.816
KY105	105	2.948	-9.882
KY106	106	2.623	-10.360
KY107	107	2.767	-9.917
KY109	109	2.816	-8.522
KY111	111	2.097	-10.026
KY113	113	2.786	-7.860
KY114	114	2.772	-8.669
KY115	115	2.736	-7.528
KY116	116	3.038	-6.324
KY117	117	2.781	-8.326
KY118	118	2.657	-7.678
KY119	119	2.362	-9.012
KY120	120	2.224	-7.461
KY121	121	2.965	-7.214
KY122	122	2.922	-6.366
KY123	123	2.987	-7.306
KY124	124	2.851	-8.823
KY125	125	2.916	-7.066
KY126	126	2.833	-7.536
KY127	127	2.395	-7.909
KY128	128	2.819	-7.198
KY129	129	2.690	-6.209
KY130	130	2.912	-4.790
KY131	131	3.001	-6.193
KY132	132	2.727	-6.717
KY133	133	2.982	-5.625
KY134	134	2.731	-8.529
KY135	135	3.175	-8.564
KY136	136	3.111	-4.380

KY137	137	2.980	-6.832
KY138	138	2.706	-8.058
KY139	139	2.529	-8.296
KY140	140	2.962	-5.458
KY141	141	2.965	-5.081
KY142	142	2.916	-4.209
KY143	143	2.210	-7.396
KY144	144	2.729	-6.486
KY145	145	2.691	-8.539
KY146	146	2.805	-9.121
KY147	147	2.331	-10.239
KY147.3	147.3	2.838	-9.399
KY148	148	2.876	-8.886
KY149	149	2.820	-8.283
KY150	150	2.552	-8.013
KY151	151	2.701	-7.294
KY152	152	2.700	-7.538
KY153	153	2.646	-7.650
KY154	154	2.094	-7.351
KY155	155	2.363	-7.876
KY156	156	2.296	-8.653
KY157	157	1.683	-7.953
KY158	158	2.005	-7.703
KY159	159	1.707	-7.154
KY161.5	161.5	3.021	-7.808
KY162	162	2.695	-8.225
KY163	163	2.953	-9.694
KY164	164	2.842	-6.932
KY165	165	2.459	-8.928
KY166	166	2.327	-9.921
KY167	167	1.938	-9.473
KY168	168	2.541	-9.154
KY169	169	2.261	-9.095
KY170	170	2.912	-8.100
KY171	171	2.896	-7.613
KY172	172	2.594	-8.586
KY173	173	2.886	-7.686
KY174	174	2.379	-8.475
KY175	175	2.596	-8.777
KY176	176	2.777	-7.994
KY177	177	1.335	-9.373
KY178	178	2.549	-8.931
KY179	179	2.133	-8.519
KY180	180	2.603	-7.439
KY181	181	1.856	-8.763
KY182	182	1.906	-7.637
KY183	183	1.674	-9.969
KY184	184	2.443	-7.003
KY185	185	2.103	-6.402
KY186	186	2.300	-6.394
KY187	187	1.514	-8.500
KY188	188	2.403	-7.670
KY189	189	2.441	-9.263
KY190	190	2.082	-9.511
KY191	191	2.733	-9.540
KY192	192	2.850	-9.645
KY192.8	192.8	2.783	-10.085

KY194	194	2.226	-9.953
KY195	195	2.548	-9.760
KY196	196	2.658	-10.785
KY197	197	2.475	-9.762
KY198	198	1.827	-9.621
KY199	199	2.045	-9.681
KY200	200	2.115	-8.269
KY201	201	2.223	-8.623
KY202	202	1.918	-9.472
KY203	203	2.027	-9.136
KY204	204	2.260	-9.757
KY205	205	0.943	-11.925
KY207	207	2.568	-9.015
KY208	208	2.327	-9.429
KY209	209	2.345	-9.959
KY210	210	2.167	-10.243
KY211	211	1.807	-10.626
KY213	213	1.593	-10.487
KY214.3	214.3	2.335	-9.735
KY215	215	2.198	-11.411
KY216	216	1.615	-11.246
KY217	217	1.862	-10.155
KY218	218	2.119	-9.736
KY219	219	1.485	-11.161
KY220	220	2.989	-8.741
KY221	221	1.343	-11.417
KY224	224	2.459	-11.075
KY225	225	1.496	-11.012
KY226	226	1.901	-9.857
KY227	227	1.987	-9.269
KY228	228	1.126	-11.993
KY228.8	228.8	2.022	-10.259
KY230	230	1.849	-9.322
KY231	231	0.945	-12.062
KY232	232	2.513	-9.533
KY233	233	2.258	-11.619
KY234	234	1.336	-11.080
KY235	235	0.956	-12.130
KY236	236	2.379	-9.474
KY237	237	1.933	-11.322
KY238	238	0.871	-10.762
KY239	239	2.154	-5.096
KY240	240	0.181	-12.179
KY241	241	1.813	-9.056
KY242	242	2.051	-9.798
KY243	243	2.064	-10.238
KY244	244	0.726	-11.169
KY245	245	2.423	-9.716
KY247	247	2.722	-8.893
KY248	248	0.727	-11.899
KY249	249	2.195	-10.415
KY250	250	0.954	-12.015
KY251	251	2.032	-8.886
KY252	252	1.306	-10.497
KY253	253	1.149	-11.372
KY255	255	1.234	-10.766
KY256	256	2.137	-9.856

KY257	257	0.798	-11.119
KY258	258	1.097	-11.314
KY259	259	1.604	-9.842
KY260	260	1.633	-9.469
KY261	261	1.388	-9.913
KY262	262	2.153	-9.823
KY263	263	2.219	-10.537
KY264	264	2.608	-8.424
KY265	265	2.452	-10.003
KY266	266	2.419	-9.472
KY267.5	267.5	2.477	-9.880
KY269	269	0.871	-10.712
KY270	270	2.016	-9.037
KY271	271	1.634	-9.074
KY272	272	1.179	-11.426
KY272.5	272.5	0.671	-8.526
KY274	274	2.371	-8.918
KY275	275	2.066	-8.286
KY276	276	1.843	-10.199
KY277	277	0.944	-8.978
KY278	278	1.795	-8.299
KY279	279	1.771	-8.308
KY280	280	1.367	-8.231
KY281	281	0.748	-8.725
KY282	282	0.556	-8.798
KY283	283	0.686	-8.107
KY284	284	1.655	-8.395
KY285	285	1.527	-8.333
KY287	287	1.229	-8.608
KY288	288	0.844	-8.861
KY289	289	0.720	-8.663
KY290	290	1.119	-9.228
KY291	291	0.434	-8.058
KY292	292	0.476	-8.179
KY293	293	1.357	-7.354
KY294	294	0.422	-11.762
KY295.5	295.5	0.337	-7.685
KY301	301	0.398	-9.192
KY302.3	302.3	0.354	-8.066
KY303	303	0.651	-8.962
KY311	311	1.709	-8.015
KY312	312	1.291	-7.967
KY312.5	312.5	1.386	-7.699
KY313	313	1.085	-6.871
KY313.6	313.6	0.845	-8.064
KY314	314	0.951	-8.515
KY314.5	314.5	1.166	-7.681
KY315	315	1.070	-6.851
KY315.5	315.5	1.431	-8.036
KY316	316	0.901	-7.757
KY316.5	316.5	0.852	-8.364
KY317	317	0.928	-7.287
KY317.5	317.5	0.519	-8.322
KY318	318	0.552	-7.752
KY318.5	318.5	0.509	-8.702
KY319	319	0.638	-9.048
KY319.5	319.5	0.600	-7.409

KY320	320	0.494	-6.904
KY320.5	320.5	0.816	-8.396
KY321	321	0.788	-7.344
KY321.5	321.5	0.149	-9.965
KY322	322	0.357	-8.989
KY322.5	322.5	0.099	-8.718
KY323	323	0.891	-7.903
KY323.5	323.5	0.401	-7.187
KY324	324	0.180	-7.800
KY325	325	0.145	-7.350
KY325.5	325.5	0.171	-7.962
KY325.8	325.8	0.464	-7.549
KY326	326	0.254	-7.770
KY326.5	326.5	0.035	-8.580
KY327	327	0.051	-8.987
KY327.5	327.5	0.302	-7.810
KY328	328	0.289	-7.873
KY328.5	328.5	0.470	-8.544
KY329	329	0.017	-7.809
KY329.5	329.5	0.307	-7.736
KY330	330	0.138	-7.716
KY330.5	330.5	-0.092	-7.960
KY331	331	-0.011	-8.056
KY331.5	331.5	0.006	-8.104
KY332	332	-0.237	-8.855
KY332.5	332.5	0.064	-8.252
KY333	333	0.027	-7.425
KY333.5	333.5	-0.105	-9.362
KY334	334	-0.605	-10.148
KY334.5	334.5	-0.335	-8.061
KY335	335	-0.650	-7.599
KY335.5	335.5	-0.622	-8.774
KY336	336	-0.620	-7.435